Structures 33 (2021) 2413–2423

Contents lists available at ScienceDirect

Structures

journal homepage: www.elsevier.com/locate/structures

Determining bond strength of seven-wire strands in prestressed concrete

Prabha Mohandoss [a,*], Radhakrishna G. Pillai [b], Ravindra Gettu [c]

[a] Assistant Professor, Department of Civil Engineering, National Institute of Technology Tiruchirappalli, India
[b] Associate Professor, Department of Civil Engineering, Indian Institute of Technology Madras, Chennai, India.
[c] V.S. Raju Institute Chair Professor, Department of Civil Engineering, Indian Institute of Technology Madras, Chennai, India

ARTICLE INFO

Keywords:
Bond strength
Pull-out
Pretensioned
Prestressed
Concrete
Compressive strength
Strand

ABSTRACT

The three mechanisms governing the strand-concrete (S-C) bond in pretensioned concrete (PTC) systems are: (i) adhesion, (ii) mechanical interlock, and (iii) friction. These mechanisms can be influenced by various parameters like the compressive strength of concrete (f_c), applied prestress (f_{ps}), and embedment length of the strand (l_e). The existing test methods for S-C systems use unstressed strands and defines bond strength (τ_b), as the stress corresponding to a slip of 2.5 mm at free end (say, $\tau_{2.5}$). The unstressed strands and $\tau_{2.5}$ approach may lead to unconservative results and significant scatter. This paper presents the experimental program on the effects of f_c (43 and 62 MPa), f_{ps} (0.1 f_{pu} and 0.7 f_{pu}), and l_e (500 and 1000 mm) on the bond stress-slip (τ-s) behaviour in PTC systems. Analysis of the results of tests on 24 specimens indicated that (i) defining the τ_b as $\tau_{2.5}$ at the free end is not suitable for PTC specimens and (ii) the $\tau_{2.5}$ at live end exhibits significant scatter and is dependent on the embedment length, l_e. Consequently, the paper proposes a conceptual model on strand-concrete bond behavior and a rational method to determine τ_b as the stress corresponding to the yield bond stress (τ_{yield}). The determined τ_{yield} is independent of f_{ps} and l_e and exhibits less scatter than $\tau_{2.5}$. Finally, the use of taut strand specimens is recommended as they are easier to prepare than stressed strand specimens, to determine τ_{yield}.

1. Introduction

In the pretensioned concrete (PTC) systems, the strand-concrete (S-C) bond plays a vital role in ensuring adequate structural performance. The S-C bond is necessary to provide not only adequate safety, but also adequate ductility [1]. The failure of the S-C bond can also lead to cracking of concrete, which can provide easy access for the deleterious elements causing premature and localized corrosion of the embedded strands. Although, state-of-the-art design procedures and construction materials/practices are available to ensure the adequate S-C bond. However, shear cracks have been observed on numerous PTC girders on an elevated highway in Mumbai, India (see Fig. 1). Also, literature reports similar shear cracks in many other PTC systems [2,3]. Such scenario necessitates a standard quality control test to determine the τ_b of PTC systems. At present, suitable standardized test methods for this are not available.

This paper evaluates various test methods in literature, presents results from a comprehensive strand pull-out test program, and develops a rational method (named as yield bond stress method) to determine the τ_b of PTC systems. Also, a conceptual model explaining the bond behavior in PTC systems is presented.

1.1. Mechanisms of strand-concrete (S-C) bond

The S-C bond in PTC systems is governed by three mechanisms: (i) adhesion, (ii) friction, and (iii) mechanical interlock [4,5]. Unlike conventional reinforced concrete (CRC) systems, due to the lubricant residue on the strand surface and the possible slip during the prestress release, the role of adhesion is minimal in the S-C bond in PTC systems [6]. In particular, at the member ends, the adhesion would be lost during prestress transfer. The friction and mechanical interlock play significant roles in the S-C bond in PTC systems [7]. Friction is provided by the concrete confinement and the wedging action is due to Hoyer effect [8]. The wedging action induces compressive stresses with a component normal to the S-C interface and enhances the friction near the ends of the member. Mechanical interlock is provided by the concrete keys formed by the helical shape of the six outer wires of the strand.

* Corresponding author.
E-mail address: prabham@nitt.edu (P. Mohandoss).

https://doi.org/10.1016/j.istruc.2021.06.004
Received 14 March 2021; Received in revised form 31 May 2021; Accepted 2 June 2021

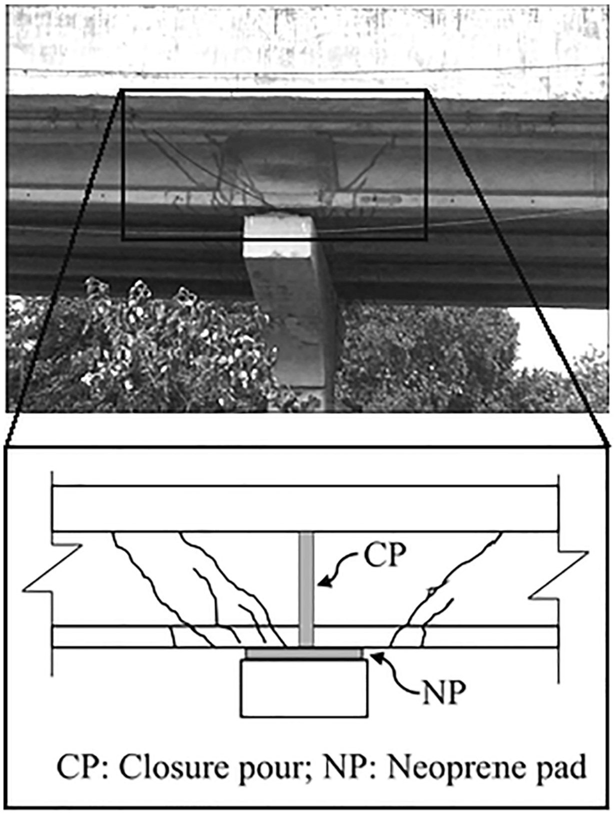

Fig. 1. Shear cracks in a highway bridge girder.

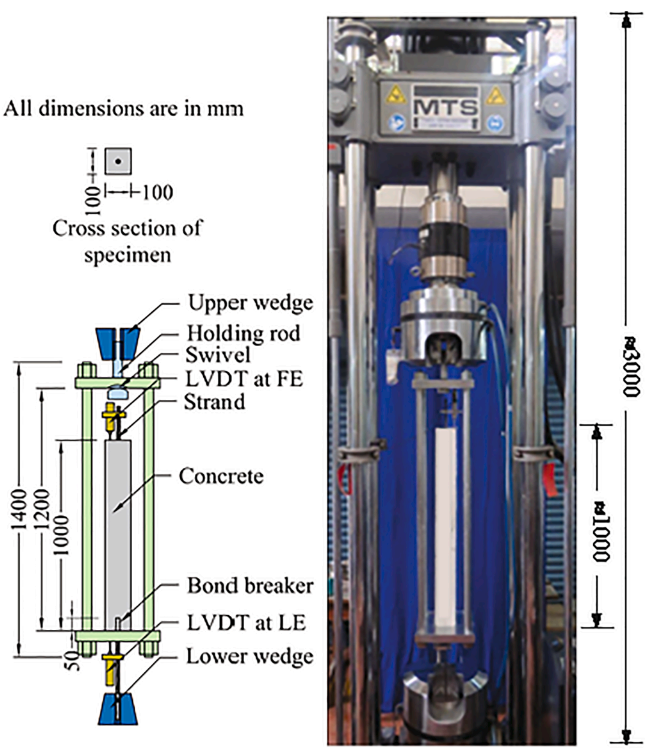

Fig. 2. A schematic illustration and photograph of the pull-out test configuration.

Table 1
Experimental program showing the test variables.

Specimen ID	Experimental variables			No. of specimens
	f_c (MPa)	l_e (mm)	f_{pi} (MPa)	
f_c43-T-Sh	43	500	0.1 f_{pu}	6
f_c62-T-Sh	62			6
f_c62-T-Lo		1000		6
f_c62-S-Lo			0.7 f_{pu}	6

Note:
$f_c$xx - Average compressive strength.
T - Taut (0.1 f_{pu}).
S - Stressed (0.7 f_{pu}).
Sh - Short l_e (500).
Lo - Long l_e (1000).

Table 2
Details of concrete mixes used.

Ingredients	Compressive strength of concrete at 28 days, f_c	
	f_c43	f_c62
Cement (kg/m^3)	380	420
Water - cement ratio	0.50	0.40
Aggregate 10 mm down (kg/m^3)	432	428
Aggregate 20 mm down (kg/m^3)	648	641
Sand, 4 mm down (kg/m^3)	750	743
Superplasticizer (% bwoc)	0.8	0.6

1.2. Definitions and formulations of bond strength

For CRC systems, *fib*-MC (1990) [9] considers the load versus slip relationship using which, the τ can be calculated as a function of slip, *s*, as follows.

$$\tau(x) = \tau_{01}\left(\frac{s(x)}{s_{01}}\right)^{\alpha} \quad (1)$$

where, τ_{01} is average bond stress corresponding to the pull-out force, P_{01} (MPa); s(x) is slip at any load × (mm); s_{01} is slip of 0.1 in (mm); and α is an exponential factor of bond stress-slip model. Based on this, Balázs (1992) [10] proposed the following equation for τ_b along the transmission zone in PTC systems.

$$\tau_b = \eta_1\eta_2 f_{ci}^{0.5}\left(\frac{s}{d_s}\right)^{\eta_3} \quad (2)$$

where, η_1 is the upper, mean, or lower bound value of τ;η_2, η_3 are empirical constants; *s* is the slip (mm); and d_s is the diameter of strand (mm). Later, EN 2 (2004) [11] and *fib*-MC (2010) [12] codes presented the following formulation for τ_b of CRC and PTC systems.

$$\tau_b = \eta_{p1}\eta_{p2}f_{ctd} \quad (3)$$

where, η_{p1} is the coefficient to account for the type of tendon, η_{p2} is the coefficient to account for the bond conditions, and f_{ctd} is the design tensile strength of concrete (MPa). Later, Dang et al. (2015) [13] adapted Eq. (1) for CRC systems given in *fib*-MC (2010) by incorporating a coefficient 'k_b' to calibrate the τ_b for strands with and without stress as follows.

$$\tau(x) = k_b\tau_{01}\left(\frac{s(x)}{s_{01}}\right)^{\alpha} \quad (4)$$

where, k_b is the calibration coefficient. However, literature does not provide sufficient guidance on how to assume values for these input parameters for other PTC systems.

The τ_b of rebar-concrete systems can be defined as the τ corresponding to a slip of 2.5 mm (say, $\tau_{2.5}$) at the free end [14,15]. In the

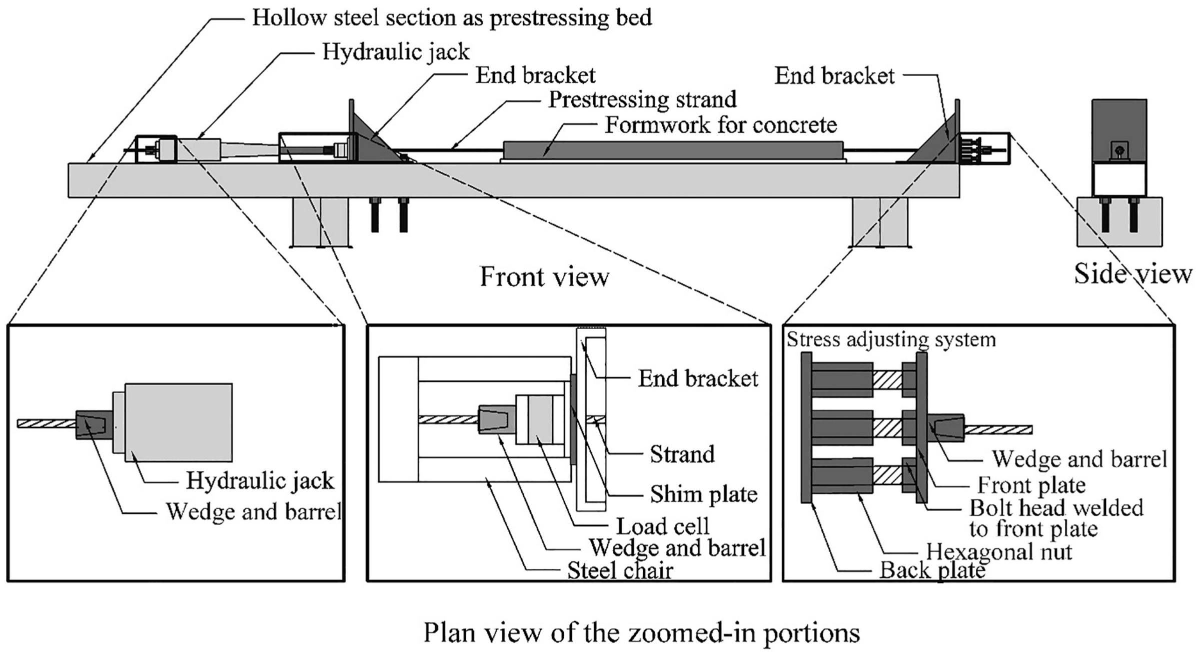

Fig. 3. Prestressing bed used to cast the specimen.

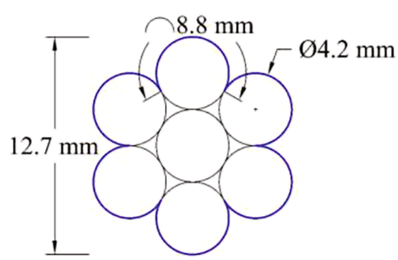

Fig. 4. Cross-section of 7 wire strand.

case of rebars, the difference in the instantaneous slips at live and free ends is negligible because the l_e is about 150 mm [16]. Also, this difference increases as a function of l_e [1,17,18]. Hence, the recommendation by ASTM A1081 (2012) [19] to define the τ_b of strand-concrete (S-C) systems as $\tau_{2.5}$ at the free end may not be appropriate [20,21]. This is because, during the pull-out test, the S-C bond deforms progressively from the live end and along the length of the embedded strand, which is typically longer than the typical pull-out specimens with rebars. Hence, the effect of l_e on the pull-out behavior and determined τ_b is significant in the case of strand specimens.

1.3. Factors influencing the S-C bond

The concrete strength (f_c) is one of the most influencing parameters, an increase in f_c can lead to an increase in its stiffness, which in turn provides more confinement - leading to improved τ_b. The τ_b of various PTC systems reported in literature shows significant scatter [22–28]. This scatter could be due to the differences in the geometry of specimens used, the prestress levels, and testing and evaluation methods.

The l_e could significantly influence the failure mode during the pull-out tests in CRC systems [18,29,30]. For PTC systems, Martí-Vargas et al. (2006) [31] and Naito et al. (2015) [32] recommended an l_e that is longer than transmission length (L_t). Later, Mohandoss and Pillai (2017) [33] suggested that l_e should be more than $2L_t$, so that the applied prestress would be effectively transferred at both ends of the test

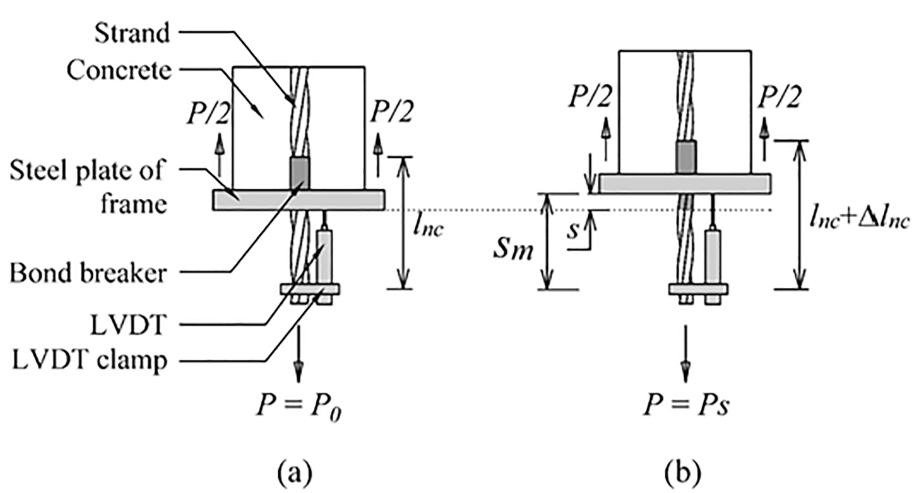

Fig. 5. Measurement of slip at live end.

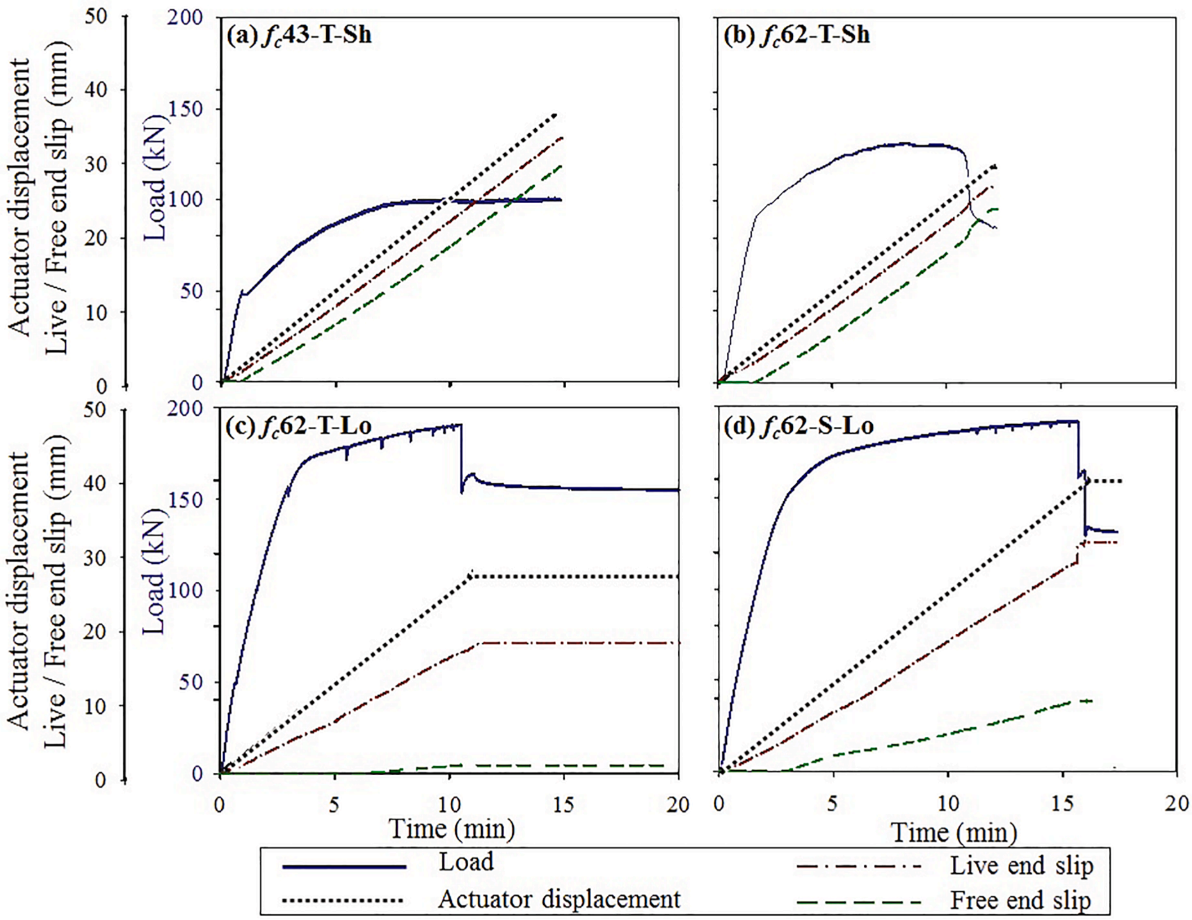

Fig. 6. Representative graphs of load, displacement, slip at free and live ends with respect to time.

specimens. Also, the initial prestress applied (f_{pi}) plays a crucial role in the S-C bond contributing to the Hoyer effect [34,35]. Naito et al. (2015) found that the stressed strands exhibited higher τ_b than unstressed strands. Also, the effect of f_{ps} on τ-s behaviour for the PTC systems is not well addressed in the literature [31,36,37]. This paper fills this knowledge gap by presenting test data on the effect of f_{ps} and l_e on τ_b of PTC systems.

1.4. Test methods to determine the bond strength (τ_b)

The widely used bond strength test methods are Moustafa pull-out test [38] ASTM A1081 (2012) [39] and ECADA test method [31]. ASTM A1081 (2012) determines the bond strength (τ_b) by using the pull-out force corresponding to 2.5 mm slip at the free end (FE) of an unstressed strand. As the strands are supplied as coils, the unstressed strand may not be perfectly straight. During the pull-out test, the strands tend to get straightened and compress the grout on concave side and also lose contact with the grout on convex side. Such uncontrolled straightening mechanisms could induce more scatter in the test results than those observed with specimens with stressed and straight strands [13]. Hence, test specimens with unstressed strands are not suitable.

To overcome such issues, Martí-Vargas et al. (2006) had proposed the ECADA test method using prestressed strands (say, $0.7f_{pu}$) to represent the in-service stress conditions. This method considers a ‘virtual part’ concept using an ‘anchorage measurement access (AMA)’ system, the stiffness of which matches with that of the concrete. As a result, this method may overestimate the τ_b [28]. Such overestimations may adversely affect the design shear strength in the transmission zone [40]. Most literature adopt large test specimens and complex test procedures, which leads to difficulties in adopting them as quality control test in the field. In short, there is a need to design a simplified test specimen and a procedure to determine the τ_b of PTC systems as an S-C interface parameter (i.e., independent of the f_{ps} and l_e of the test specimen) and avoids overestimation.

2. Research significance

Failure of the strand-concrete (S-C) bond has been observed in pretensioned concrete (PTC) bridges. The available test methods to determine the τ_b in PTC systems have limitations in terms of (i) specimen configuration and test setup, (ii) test procedure and method of evaluation, and (iii) dependence on the prestress and embedment length. This paper proposes the use of a simplified test specimen that can be cast at site and transported to the laboratory for testing, along with a new method to rationally estimate τ_b. The paper also presents a conceptual model for S-C bond behavior that can be helpful to develop constitutive models.

3. Experimental program

Fig. 2 presents the experimental setup, where two LVDT’s are placed at Live end (LE) and Free end (FE), respectively, to measure the slip of the strand. Table 1 shows details of 24 pull-out specimens, each with a cross-section of (100 × 100) mm size and an embedded steel strand. The high strength, low-relaxation, seven-wire strands with 12.7 mm diameter and meeting the ASTM A416 (2016) [41] specifications were used. The modulus of elasticity and ultimate tensile strength (f_{pu}) of the strand were 198 ± 3 GPa and 1877 ± 3 MPa, respectively. Concretes with

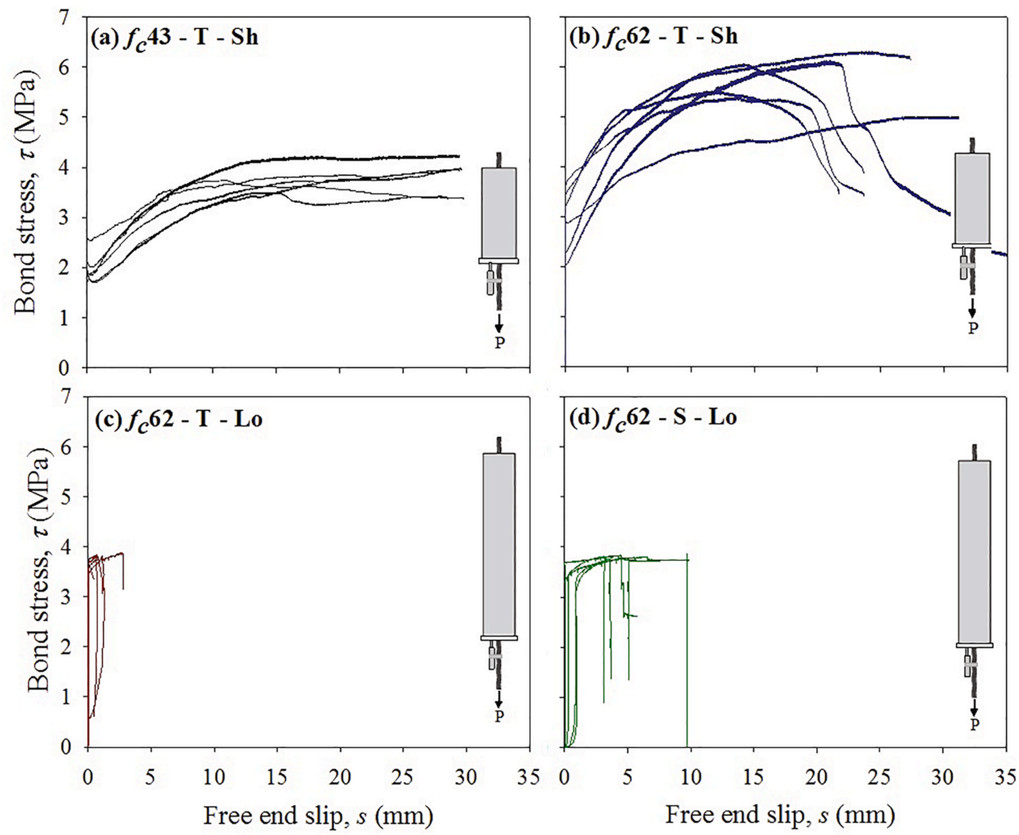

Fig. 7. Bond stress - slip at free end behavior.

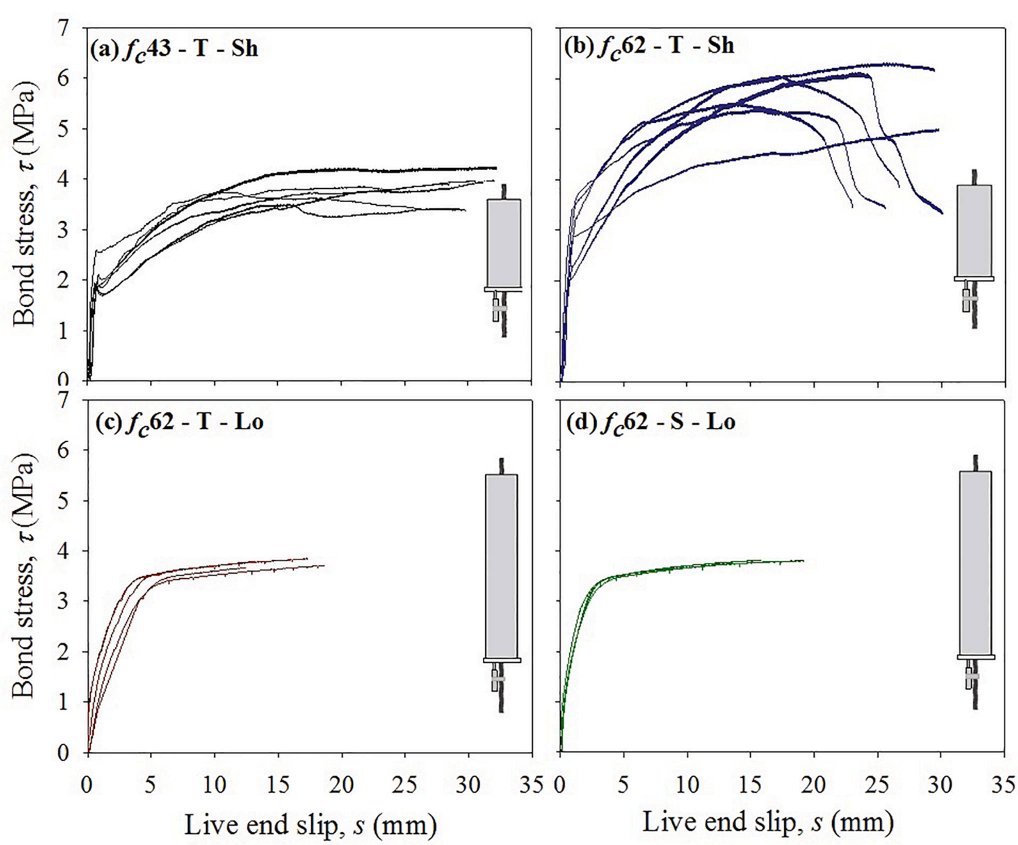

Fig. 8. Bond stress - slip at live end behavior.

Table 3
Observed τ_b of taut and stressed strands embedded in concrete.

Specimen ID	Compressive strength of concrete at testing (f_c) in MPa	Maximum bond load (P_{max}) in kN	Bond strength (τ_b) MPa		
			$\tau_{2.5}$ at FE	$\tau_{2.5}$ at LE	0.9 τ_{yield} at LE
f_c43-T-Sh-1	44.1	101	2.58	2.30	1.81
f_c43-T-Sh-2	43.8	93	2.39	2.24	1.72
f_c43-T-Sh-3	43.7	95	2.06	1.92	1.72
f_c43-T-Sh-4	42.9	94	2.57	2.38	1.75
f_c43-T-Sh-5	44.5	95	2.04	1.91	1.73
f_c43-T-Sh-6	42.3	89	2.86	2.67	1.85
f_c62-T-Sh-1	63.1	119	3.31	3.07	2.61
f_c62-T-Sh-2	61.8	132	4.28	3.97	3.28
f_c62-T-Sh-3	60.2	150	4.39	3.94	3.05
f_c62-T-Sh-4	60.4	131	4.48	3.85	2.93
f_c62-T-Sh-5	61.6	145	3.20	2.75	2.16
f_c62-T-Sh-6	62.2	144	3.65	3.02	2.06
f_c62-T-Lo-1	63.4	194	3.86	2.42	3.07
f_c62-T-Lo-2	64.7	179	–	3.09	3.08
f_c62-T-Lo-3	61.2	191	–	2.65	3.10
f_c62-T-Lo-4	63.9	189	–	2.26	3.09
f_c62-T-Lo-5	62.5	191	–	2.20	2.97
f_c62-T-Lo-6	63.1	190	–	2.96	2.95
f_c62-S-Lo-1	65.8	192	3.50	3.12	3.10
f_c62-S-Lo-2	63.5	194	3.66	3.21	3.06
f_c62-S-Lo-3	62.6	191	3.77	3.10	3.04
f_c62-S-Lo-4	62.8	190	3.64	3.18	3.04
f_c62-S-Lo-5	62.3	189	3.66	3.02	3.11

average 28-day compressive strengths (f_c) of 43 and 62 MPa were used. Table 2 provides the mixture proportions of two concretes used in this study. Specimens with prestress levels of 0.1 f_{pu} and 0.7 f_{pu} were prepared and *such strands with stress levels are denoted herein, as taut and stressed strands, respectively*. For a stress of about 0.7 f_{pu}, the L_t in concrete with $f_c \approx 62$ MPa is about 440 mm [40]. Hence, the l_e of all the stressed strand specimens were kept at 1000 mm - to ensure that l_e is more than twice the L_t, as recommended by Marti-Vargas et al. (2012) and Mohandoss et al. (2018b) [26,42]. The correlation between the τ_b of stressed and taut strands were also assessed experimentally.

3.1. Preparation of pull-out specimens

3.1.1. Initial pre-stressing

Fig. 3 shows the 6 m long and rigid prestressing bed used to cast the PTC pull-out specimens. A strand was inserted through holes on the end brackets and stressed using a hydraulic jack (with a capacity of 300 kN). Before placing the wedges and stressing the strand, a 50 mm long PVC pipe was kept around one end of the strand (as a bond-breaker) to avoid the stress concentration at the end of the specimen during the pull-out test. This end of the specimen, where load would be applied is called the live end (LE), and the other end is denoted as the free end (FE). The wedges and barrels were placed on the outer face of the end brackets in order to lock and maintain the applied stress. The pressure gauge attached with the hydraulic jack was calibrated with a ring load cell (with a capacity of 500 kN) and then the applied axial stress on the strand was calculated.

3.1.2. Casting of concrete and prestress release

Concrete was prepared and placed inside the prism moulds kept on the prestressing bed. The concrete was placed in single layer to the depth of the specimen (100 mm) and compacted by rodding as per ASTM C192 (2016) [43] especially along the horizontal S-C interface. Also, care was taken to keep the end faces of the specimens perpendicular to the axis of the strand. These are essential to ensure uniform load distribution on the concrete face at the LE and gradual stress transfer along the axis of the strand during the pull-out test. Three companion cube specimens were cast and the f_c at the time of the pull-out test was determined. The taut

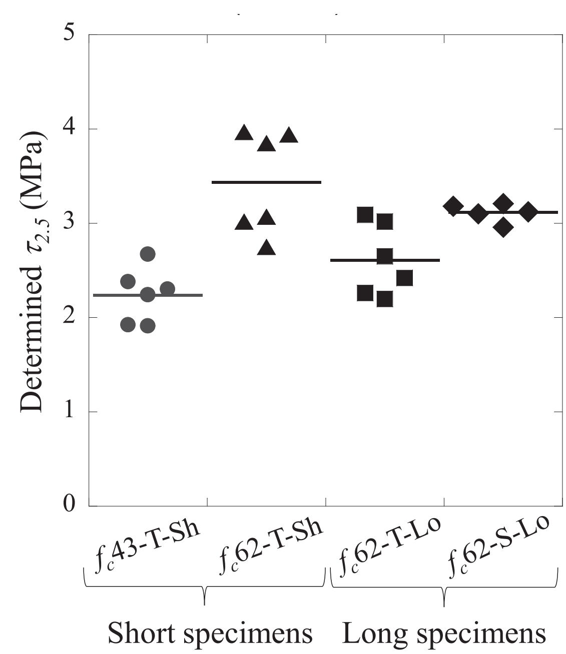

Fig. 9. Determined $\tau_{2.5}$ at live end.

specimens were demoulded and the prestress was released after 24 h. The stressed specimens were demoulded and the prestress was released only after the third day of casting, after ensuring that the concrete attained sufficient strength (say, about 60% of its target strength). The average compressive strength of concrete at transfer is 28 MPa and 40 MPa, respectively for f_c43 and f_c62 concrete. As shown in Fig. 3, a stress adjusting system with a nut-bolt arrangement was placed at the releasing end to facilitate the gradual release of prestress. The gradual releasing method was followed because it results in shorter L_t as well as similar L_t at both live and free end of the specimens [44].

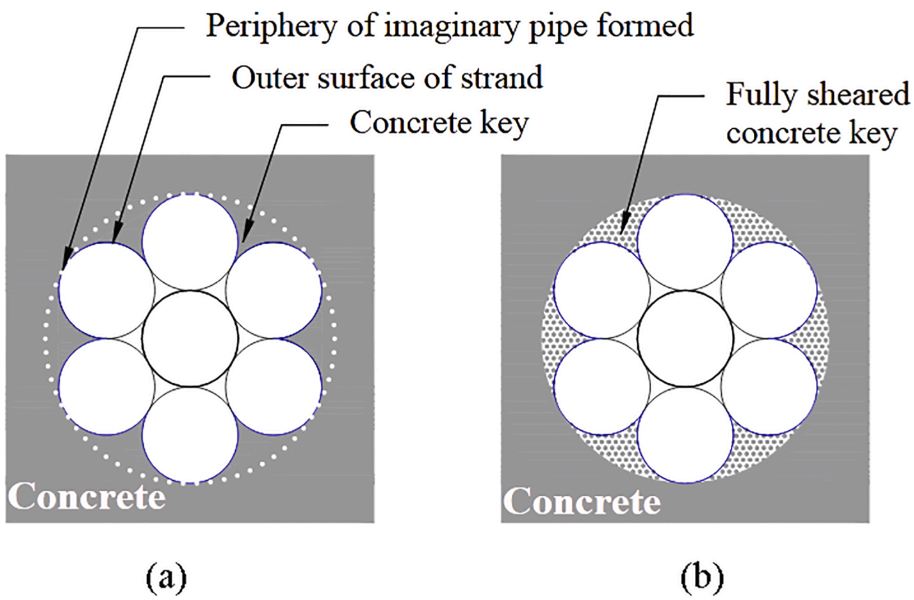

Fig. 10. S-C interface and bond failure mechanisms.

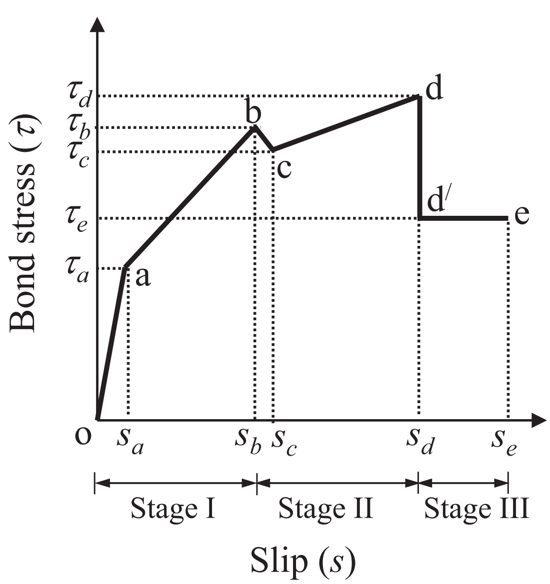

Fig. 11. Model form for the bond stress-slip behaviour.

3.2. Pull-out test set-up and procedure

A pull-out frame of 1.4 m long was designed and fabricated (see Fig. 2). The top plate of the frame was connected to a rod (with swivel joint), which was gripped at the upper wedge of the universal testing machine (UTM) (movable end). As shown in Fig. 2, the strand protruding from the live end of the specimens was inserted through the hole at the centre of the lower plate of the frame and gripped using the lower wedges of the UTM (fixed end). Two LVDTs were attached to the strand portions at the live and free ends of the specimen to measure the slips. The load was applied at a displacement rate of 2 mm/min.

The τ-s behaviour was obtained by capturing the applied load and the total slip measured (s_m) by LVDTs. The bond stress (τ) is computed by assuming a uniform average stress distribution over the embedded length (l_e) of the strand in concrete, as follows using Eq. (5)

$$\tau = \frac{P}{pl_e} \tag{5}$$

Perimeter (p) is calculated as the sum of the arc lengths of six outer wires (representing the area in conctact with the concrete). The thick line in the Fig. 4 indicates this perimeter. The diameter of the outer wires is 4.2 mm. For the 12.7 mm diameter strand used in this study, the arc length of outer wire is 8.8 mm; p is 52.8 mm and the embedment length (l_e) of the strand in concrete is 450 mm for short specimen and 950 mm for long specimens.

Fig. 5 shows a schematic illustration of the movement at the live end. As soon as the load is applied, the $l_{\rm nc}$ (length of non-contact) portion of the strand is stretched and the strand portion inside the concrete starts slipping. Hence, the true slip at the live end, s, is calculated by subtracting Δl_{nc} from s_m, where, Δl_{nc} is the elongation of the $l_{\rm nc}$ region, s_m is the net slip measured by LVDT. Thus, the true τ-s curves were obtained to determine τ_b. In this study, the following conventional and proposed definitions of bond strength (i.e., $\tau_{2.5}$ and τ_{yield}) are used.

- $\tau_{2.5}$ – average bond stress along the embedment length corresponding to 2.5 mm slip
- τ_{yield} - average bond stress along the embedment length at yield load point

4. Results and discussions

4.1. Bond strength as a function of slip at free and live ends

Fig. 6 shows the applied load (P), displacement, slips at free and live ends as a function of time and indicates the difference in the applied load required to initiate slipping at live and free ends for the four cases of (i) taut-short [T-Sh] specimens with f_c43, (ii) taut-short specimens with f_c62, (iii) taut-long [T-Lo] specimens with f_c62, and (iv) stressed-long [S-Lo] specimens with f_c62. The longer the l_e, the better the friction; hence, the larger will be the load required to cause the same slip at both live and free ends. Also, as expected, in all the four cases (a, b, c, and d) slipping at free end (dashed curve) was observed only after the yield region - indicated by the increase in slope of dashed curve happening at the same time when the slope of solid curve decreases significantly. In the case of short specimens with lower f_c, the failure mode was slipping/piping and the testing was stopped at about 15 min; whereas strands fractured in the other three cases.

Fig. 7 and Fig. 8 show the τ-s behaviour of taut and stressed strands in concrete at free end and live end, respectively. In case of long specimens,

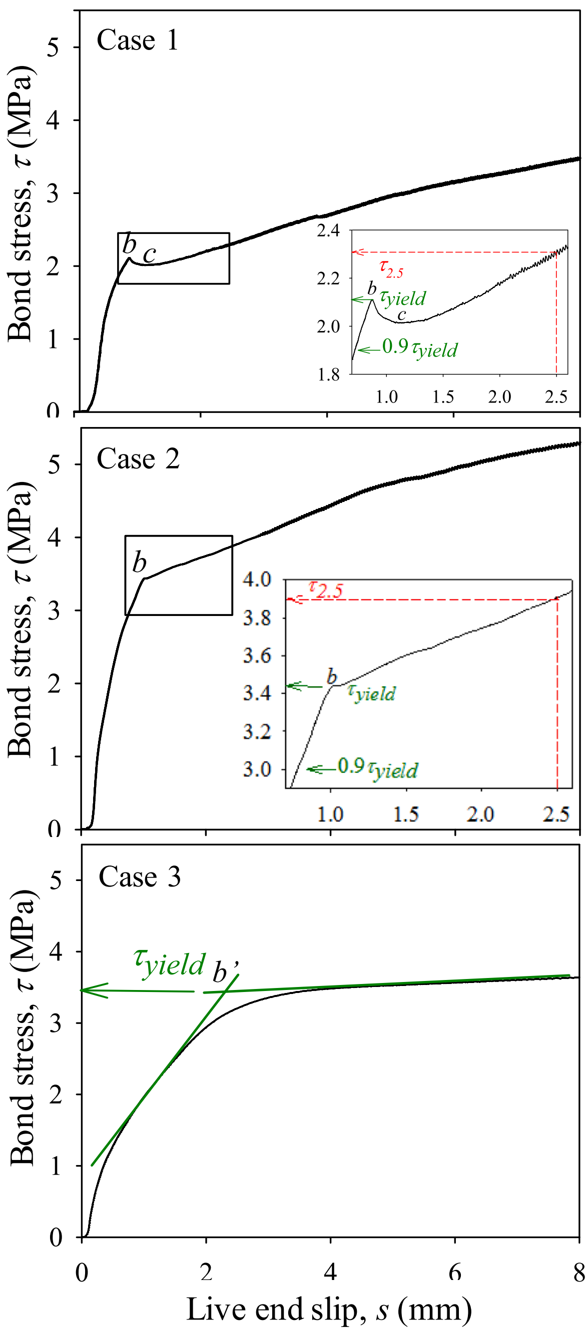

Fig. 12. Determination of τ_b using the yield bond stress method and conceptual bond stress variation along the length of the member.

the strand portion at the free end started slipping only after the yield load region (see Fig. 7 (c)); hence, $\tau_{2.5}$ at free end could not be determined. On the other hand (Fig. 8), the strand portion at live end started slipping before the yield region. The observed τ_b of taut and stressed strands embedded in concrete is reported in Table 3.

As shown in Fig. 9, in case of taut-short specimens, when comparing the cases with f_c 43 and 62 MPa, about 50% increment in $\tau_{2.5}$ was observed due to the higher stiffness of concrete. In Fig. 9, it can be seen that the determined $\tau_{2.5}$ exhibits significant scatter in case of taut strands in both 43 and 62 MPa strength concretes. The f_c62-T-Lo and f_c62-S-Lo indicate that $\tau_{2.5}$ increases by about 15%, when the stress level increases from 0.1 to 0.7 f_{pu}. Also, the results indicated that when the l_e of strand increases from 500 to 1000 mm, the value of $\tau_{2.5}$ decreases significantly by about 25%. This indicates that $\tau_{2.5}$ is dependent of l_e. Hence, unlike conventional reinforced concrete systems, the slip method cannot be used for pretensioned concrete systems. This is because the l_e in case of prestressed strands depends on the L_t of the specimen, which in turn depends on the prestress level f_{ps} and the strength of concrete. This necessitates a rational approach, based on the τ-s behaviour, to determine τ_b as an S-C interface parameter that is independent of f_{ps} and l_e.

4.2. Bond stress-slip (τ-s) behavior of S-C systems - a conceptual model

To understand the bond behaviour, Fig. 10 shows the bond failure mechanisms at the S-C interface with concrete keys. The dotted circle in Fig. 10(a) indicates the ‘fictitious pipe’ formed by the locus of the outermost points of the six wires of the strand along the length. The concrete keys are formed due to helical shape of the six outer wires of the strand. Fig. 10(b) indicates the scenario of complete shear failure (due to pull out) along the ‘fictitious pipe’. Further details regarding this are given later.

Based on the observed behaviour (Fig. 6 and Fig. 8), a conceptual model was developed to explain the bond behaviour at S-C interface, see Fig. 11. The τ-s behaviour can be divided into three stages as follows:

- Stage I - Elastic stage (‘o’ to ‘b’)
- Stage II - Progressive bond degradation stage (‘b’ to ‘d’)
- Stage III - Post-peak failure stage (‘d’ to ‘e’)

Stage I includes the region with bi-linear behavior (from ‘o’ to ‘a’ and ‘a’ to ‘b’) due to the frictional resistance due to the Hoyer effect and concrete confinement. The change in stiffness before and after Point ‘a’ could be due to the initiation of micro cracking along the ‘fictitious pipe’. The concrete keys can be assumed to be intact during this stage. Point ‘b’ indicates the yield bond stress (τ_{yield}), where the slope decreases due to the loss of friction and marks the end of Stage I.

Stage II starts with the loss of friction, slipping, and corresponding stress release along the fictitious pipe resulting in a reduction in the bond stress from τ_b to τ_c (from Point ‘b’ to ‘c’). Upon further loading (from Point ‘c’ to ‘d’), the crushed or loose particles at the interface get compressed and densified. During this stage, the mechanical interlock plays a significant role and gives further resistance to slip, which increases the bond stress after yield (from Point ‘c’ to ‘d’). With increase in load, the bond degrades and concrete keys get damaged progressively from the live end towards the free end.

Beyond Stage II, the concrete keys were fully sheared due to increasing load, as shown in Fig. 10(b), and creates a smooth cylindrical path like a pipe for the strand to slip freely leading to pull-out failure. This indicates the debonding at Point d. Thus, the bond stress dropped from d to d′ as the strand could freely slip. However, there would be a slight friction between the strand and concrete after the mechanical bond failure. Due to this skin friction at the S-C interface, the curve does not approach zero stress level.

For short specimens with high and low strength concrete, all three stages were captured experimentally. However, for some specimens, Stage III was not captured as the strand slipped beyond the capacity of the LVDTs used. Stage III cannot be seen in long specimens (see Fig. 8 (c) and (d)) as the longer l_e provides more resistance to slip - resulting an average maximum load of about 190 kN. At this point, strands got ruptured as the applied load reached the breaking load of strand, before the formation of a pipe at the S-C interface. Stage I, II, and III were observed in short specimens and only Stage I and II were observed in long specimens. Therefore, only the Stage I and II were considered hereafter for the analysis.

4.3. Determination of τ_{yield}

The yield regions on the τ-s curves (see Fig. 12) were observed in three cases.

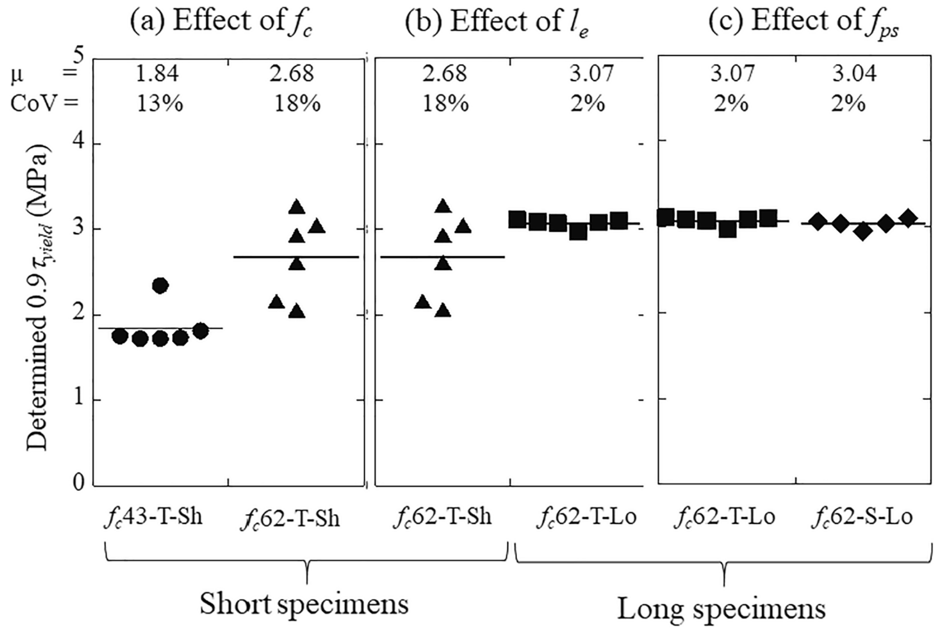

Fig. 13. Determined 0.9τ_{yield}.

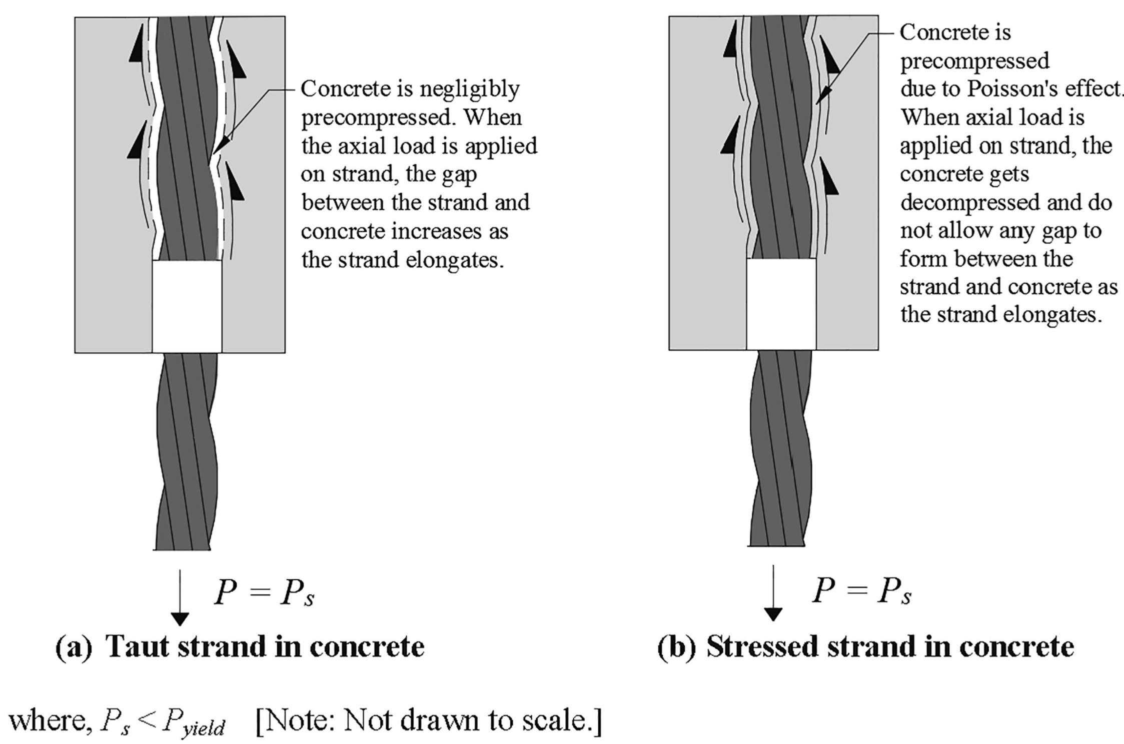

Fig. 14. Changes at the S-C interface during the pull-out test (until τ_{yield}).

- Case 1: A point on the curve indicating a sudden change in slope followed by a reduction in bond stress
- Case 2: A point on the curve indicating a sudden change in slope without any reduction in bond stress
- Case 3: A region on the curve with a gradual and significant change in slope.

Case 1 and 2 were observed in the specimens with the short taut strands in concretes. The inserts in Fig. 12 (a) and (b) show the close-up views near the yield point for these cases. As explained in the conceptual model, in Case 1, the bond stress increases till Point 'b' and yield occurs. After yield, the bond stress reduces (towards Point 'c' in the close-up view of Fig. 12 (a)) and the bond stress increases from Point 'c' (i.e., the curve moves upwards). Case 1 with a significant drop at Point 'b' was observed in the short taut strand specimens embedded in low strength concrete (f_c = 43 MPa). On the other hand, no significant drop at Point 'b' was observed in Case 2. This could happen in concretes with high stiffness, where once the friction is lost, the concrete keys may not experience significant compression. Further, the curve starts moving upward right after Point 'b' due to mechanical interlock. As a result,

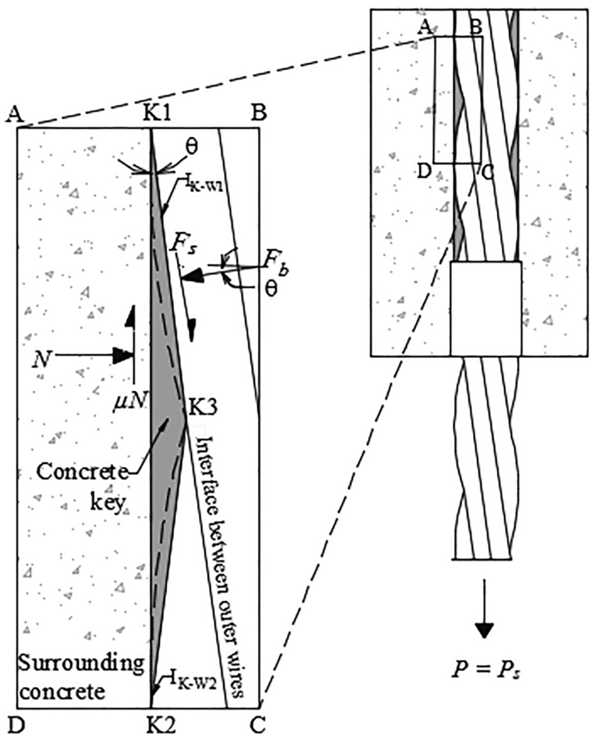

Fig. 15. Mechanism of bond failure at S-C interface.

Case 2 was observed in the short taut strand specimens with high strength concrete (f_c = 62 MPa). Case 3 was typically observed in long specimens with both taut and stressed strands embedded in high strength concrete (f_c = 62 MPa). The S-C interface gradually yields as shown in Fig. 12 (c) and the yield region was determined as a point, where the parallel line of each region meets (pre and post yield portions) and stress corresponding to that point is considered as τ_{yield}. To be conservative, this study defines τ_b of PTC systems as 90% of τ_{yield} (i.e., $\tau_b = 0.9\tau_{yield}$), herein.

4.4. Effect of f_c, f_{ps}, and l_e on τ_{yield}

Fig. 13 (a) indicates that when f_c increased from 43 to 62 MPa, τ_{yield} increased by about 30%, which is expected due to increased stiffness and confinement of concrete. Fig. 13 (b) shows the determined $0.9\tau_{yield}$ of the taut and stressed strands in concrete with l_e = 500 and 1000 mm. As the yield attained before the strands experienced 2.5 mm slip (see Fig. 8(a)), the τ_{yield} was lower than the $\tau_{2.5}$ for these cases. Fig. 8 (a) and (b) also showed that the τ_{yield} of taut strands (with l_e = 500 mm) was about 20% greater than its $\tau_{2.5}$. Comparison of data in Fig. 13 (b) and (c) indicate that τ_{yield} would remain the same irrespective of the l_e of the strands, although with a larger scatter in case of short strands. In case of long specimens (l_e = 1000 mm) with f_c = 62 MPa (see Fig. 13 (c)), τ_{yield} was similar for the taut and stressed strands (i.e., 3 MPa). This indicate that the τ_{yield} method could eliminate the effect of f_{ps} on the determined τ_b. In short, a rational method to determine τ_b irrespective of l_e is developed.

The obtained values of τ_b ($0.9\tau_{yield}$) were compared with $\tau_{2.5}$ reported in literature. For the taut strands, the value of average τ_b (2.68 MPa) was comparable with τ_b of unstressed strands in concrete obtained using Moustafa's and ASTM test methods and reported in Rose and Russell (1997) and Dang et al. (2015), respectively. Similarly, for the stressed strands, the value of average τ_b (i.e., 3 MPa) is comparable with the τ_b of strands in concrete obtained using ECADA test method and reported in Martí-Vargas et al. (2013b). As the proposed τ_{yield} is comparable with the τ_b of PTC system in the literature, τ_{yield} method can be used to get τ_b as an SC parameter independent of f_{ps} and l_e.

4.5. Bond failure mechanism in PTC systems

The τ-*s* behaviour of the taut and stressed strands is different at the S-C interface due to the applied f_{ps} and Hoyer effect. To illustrate this mechanism, changes at the interface near the live end of the specimen during the pull-out test is shown in Fig. 14. During the pull-out test, when $P_s < P_{yield}$, strand at the interface deforms elastically and gets debonded from the surrounded concrete. The Hoyer effect is found to be insignificant in the taut strand specimens, where the applied f_{ps} is minimal (about 0.1 f_{pu}), thus the induced precompression in the concrete is negligible. The dashed lines in Fig. 14 (a) indicate the outer surface of the taut strand in contact with concrete. The unshaded region in the figure shows the debonded region (gap between the strand and concrete). On the contrary, in the stressed strand specimens, the Hoyer effect would be significant, which precompresses the surrounding concrete at the transfer of applied f_{ps} (about 0.7f_{pu}). As a result, while the strand elongates under the load, the surrounding concrete gets decompressed due to elasticity, which prevents the debonding of strand from the surrounding concrete (Fig. 14 (b)). The decompressed concrete gives more stiffness and resistance to slip, whereas, in the taut strand specimens, the concrete would not experience such resistance and would debond when the strand elongates. Hence, there is no restrain for the strand movement, and the strand starts slipping once the load is applied. The significance of this mechanism is clearly seen in Fig. 8 (c) and (d), which display the τ-*s* behaviour of taut and stressed strands in concrete. This implies that the Hoyer and Poisson's effects at transfer and loading play a critical role on the S-C bond in the Stage I. After yield, Stage II would be similar for both taut and stressed strand specimens.

Fig. 15 displays the mechanism of bond failure at the S-C interface. A close-up of the region ABCD indicates the forces acting on the concrete keys under loading. I_{K-W1} and I_{K-W2} represent the interfaces between the concrete key and the outer wires shown. When the load is applied, the strand tends to slip. This activates the friction and mechanical interlock mechanisms and induces the shear force (F_s) and bearing force (F_b) on the interface between the concrete key (typically the cement paste with fine aggregates) between the outer wires of the strand.

The following assumptions are made in developing the bond failure mechanism: (i) the curved region (dashed line) of outer wire is considered as a straight line for simplification and the triangle formed by the points K1, K2, and K3 forms the concrete key and (ii) there is no relative movement between the outer wires - indicating no resistance offered by the I_{K-W2} interface. Also, note that in PTC elements, the strands exhibit complete pull-out failure due to shearing of the concrete keys. At the S-C interface, when the strand starts slipping, the surrounding concrete resists the movement of the strand and induces the normal force (*N*) and frictional force (μ*N*) on the outer surface of the concrete key (K1-K2). Therefore, to be in equilibrium, the sum of the forces acting in the vertical and horizontal direction is zero as given Eqs. 6 and 7.

$$\sum F_x = 0;\ N - F_b \cos\theta + F_s \sin\theta = 0 \tag{6}$$

$$\sum F_y = 0;\ \mu N - F_b \sin\theta - F_s \cos\theta = 0 \tag{7}$$

As the test or pulling progresses, with the increase in applied load, the shear force at the interface increases; when the ($F_s \sin\theta + F_b \cos\theta$) > μ*N*, the concrete key region (K1-K2-K3) gets sheared (along K1-K2) and forms a pipe for the strands to slide. Consequently, this failure facilitates the free movement of the strands and the concrete keys along the interface K1-K2 surface (complete pull-out failure). This indicates (as discussed earlier) that the f_{ps} plays a role on the slope of the initial region of the τ-s plot (say, up to yield point); but not on the yield point or τ_b. Therefore, the load required to fail the concrete keys is same irrespective of the slip of the strand. Thus, the bond failure of the PTC members depends on the failure of the concrete keys between the wires, which is a function of the mechanical properties of concrete and the interlocking effects due to the shape of the concrete keys/helical strands.

5. Conclusions

This study emphasizes that the existing test methods to determine the bond strength (τ_b) in rebar-concrete systems cannot be used for strand-concrete systems (say, PTC systems) because of the associated prestress and the definition of τ_b as stress at 2.5 mm slip. To develop a suitable test procedure, pull-out specimens of different length and prestress levels were tested. The results concluded that existing 2.5 mm slip method is not suitable for determining the τ_b of PTC systems, as τ_b becomes a function of f_{ps} and l_e. Based on the bond stress-slip (τ - s) behavior obtained for specimens with different compressive strength (f_c), prestress (f_{ps}), and embedment length (l_e), this study proposes a new method to determine τ_b using yield bond stress (τ_{yield}) obtained from the τ - s graph. The determined τ_{yield} is independent of the applied f_{ps} and l_e and similar for both taut and stressed strands (about 3 MPa). Hence, it is concluded that the taut strand specimens can be used to determine the τ_b of PTC systems; and hence, the complexity in determining the τ_b of PTC systems can be reduced. Also, it was concluded that the failure of strand-concrete depends on the failure of concrete keys, which is a function of shear strength of concrete and interlocking effects due to the helical shape of the strands.

Declaration of Competing Interest

The authors declare that they have no known competing financial interests or personal relationships that could have appeared to influence the work reported in this paper.

References

[1] fib (International federation for structural concrete) (2000) Bond of reinforcement in concrete. State of the art report. fib Bulletin no. 10, Lausanne, Switzerland.
[2] Tadros, M. K., Badie, S. S., Tuan, C. Y. (2010). Evaluation and Repair Procedures for Precast/Prestressed Concrete Girders with Longitudinal Cracking in the Web. National Cooperative Highway Research Program , NCHRP Report 654, Transportation Research Board, Washington, DC.
[3] Bullock, W.O., Barnes R. W., and Schindler A. K. (2011). Repair of Cracked Prestressed Concrete Girders, I-565, Huntsville, Alabama. Research Report No. 2F for ALDOT Project 930-601, Highway Research Center, Auburn, Alabama.
[4] Janney JR. Nature of bond in pre-tensioned prestressed concrete. J Am Concr Inst 1954;25(9):717–36.
[5] Hanson NW, Kaar PH. Flexural bond test of pretensioned prestressed beams. J Am Concr Inst 1959;55(51):783–802.
[6] Barnes RW, Grove JW, Burns NH. Experimental assessment of factors affecting transfer length. ACI Struct J 2003;100(6):740–8.
[7] Vázquez-Herrero C, Martínez-Lage I, Martínez-Abella F. Transfer length in pretensioned prestressed concrete structures composed of high performance lightweight and normal-weight concrete. Eng Struct 2013;56:983–92.
[8] Hoyer E, Friedrirch E. Beitrag zur frage der haftspannung in eisinbeton bautellin. Beton Und Eiren 1939;50:717–36.
[9] fib (International federation for structural concrete). Model code for concrete structures. Switzerland: Lausanne; 1990.
[10] Balazs GL. Transfer control of prestressing strands. PCI J 1992;37(6):60–71.
[11] European Standard (2004) EN 1992-1-2:2004: Design of concrete structures - Part 1-1: General rules and rules for buildings. European Committee for standardization (CEN) (Vol. 1). Brussels, Belgium.
[12] fib (International federation for structural concrete). Model code for concrete structures. Switzerland: Lausanne; 2010.
[13] Dang CN, Floyd RW, Murray CD, Hale WM, Martí-Vargas JR. Bond stress-slip model for 0.6 in. (15.2 mm) diameter strand. ACI Struct J 2015;112(5):625–34.
[14] BIS (Bureau of Indian Standards) IS 2770 (1967) - Part 1: Methods of testing bond in reinforced concrete, Part 1 Pull-out test. Bureau of Indian Standards, New Delhi, India.
[15] RILEM TC. RILEM recommendations for the testing and use of construction materials, RC 6 bond test for reinforcement steel. 2. Pull-out test. E & FN SPON 1983;1994:218–20.
[16] Khayat KH. Use of viscosity-modifying admixture to reduce top-bar effect of anchored bars cast with fluid concrete. ACI Mater J 1998;95(2):158–67.
[17] Abrishami HH, Mitchell D. Analysis of bond stress distributions in pullout specimens. J Struct Eng 1996;122(3):255–61.
[18] Benmokrane B, Tighiouart B, Chaallal O. Bond Strength and Load Distribution of Composite GFRP reinforcing bars in concrete. ACI Mater. J. 1996;93(3):246–53.
[19] ASTM A1081. Standard Test Method For Evaluating Bond Of Seven-Wire Steel Prestressing Strand. West Conshohocken, PA, USA: ASTM international; 2012.
[20] Dang CN, Murray CD, Floyd RW, Hale WM. Correlation of strand surface quality to transfer length. ACI Struct J 2014;111(5):1245–52.
[21] Dang CN, Murray CD, Floyd RW, Micah Hale W, Martí-Vargas JR. Analysis of bond stress distribution for prestressing strand by standard test for strand bond. Eng Struct 2014;72:152–9.
[22] Abrishami H, Mitchell D. Bond characteristics of pretensioned strand. ACI Mater J 1993;90(3):228–35.
[23] Brearley LM, Johnston DW. Pull-out bond tests of epoxy-coated prestressing strand. J Struct Eng 1990;116(8):2236–52.
[24] Cousins TE, Johnston DW, Zia P. Development length of epoxy-coated prestressing strand. ACI Mater J 1990;87(4):309–18.
[25] Haq M. Effect of self consolidating concrete (SCC) Mix proportioning on transfer and development length of prestressing strands. MS thesis. MI, USA: Michigan State University; 2005.
[26] Martí-Vargas JR, Serna P, Navarro-Gregori J, Pallarés L. Bond of 13 mm prestressing steel strands in pretensioned concrete members. Eng Struct 2012;41: 403–12.
[27] Martí-Vargas, J. R., Caro, L. A., and Serna, P. (2013a). Experimental technique for measuring the long-term transfer length in prestressed concrete. Strain, 49(2): 125-134.
[28] Martí-Vargas JR, Serna P, Hale WM. Strand bond performance in prestressed concrete accounting for bond slip. Eng Struct 2013;51:236–44.
[29] Tastani SP, Pantazopoulou SJ. Reinforcement and Concrete Bond: State Determination along the Development Length. J Struct Eng 2013;139(9):1567–81.
[30] Bakis CE, Uppuluri VS, Nanni A, Boothby TE. Analysis of Bonding Mechanisms of Smooth and Lugged FRP rods embedded in concrete. Compos. Sci. Technol. 1998; 58(8):1307–19.
[31] Martí-Vargas JR, Serna-Ros P, Fernandez-Prada MA, Miguel-Sosa PF. Test method for determination of the transmission and anchorage lengths in prestressed reinforcement. Mag Concr Res 2006;58(1):21–9.
[32] Naito C, Cetisli F, Tate T. A method for quality assurance of seven-wire strand bond in portland cement concrete. PCI J. 2015;60(4):69–84.
[33] Mohandoss P. and Pillai R. G. (2017). Effect of prestress on the bond strength of pretensioned concrete systems. International conference on Advances in construction materials and systems, 71st RILEM WEEK and ICACMS, Chennai, India, 4: 153-160.
[34] Dang, C. N., Murray C. D., Hale W. M., and Martí-Vargas, J. R. (2013). A review of factors influencing strand bond. PCI Convention and National Bridge Conference, Texas, USA, 1–15.
[35] Ramirez-Garcia AT, Dang CN, Hale WM, Martí-Vargas JR. A higher-order equation for modeling strand bond in pretensioned concrete beams. Eng Struct 2017;131: 345–61.
[36] Deng Y, Morcous G, Ma ZJ. Strand bond stress slip relationship for prestressed concrete members at prestress release. Mater Struct 2015. https://doi.org/10.1617/s11527-015-0546-1.
[37] Shin H, Lee S, Yoo D. Bond behavior of pretensioned strand embedded in ultrahigh performance fiber-reinforced cocnrete. Int J Concr Struct Mater 2018. https://doi.org/10.1186/s40069-018-0249-4.
[38] Rose DR, Russell BW. Investigation of standardized tests to measure the Bond Performance. PCI J 1997;44(4):56–80.
[39] Riding KA, Peterman RJ, Polydorou T. Establishment of minimum acceptance criterion for strand bond as measured by ASTM A1081. PCI J 2014;61(3):86–103.
[40] Mohandoss P, Pillai RG, Sengupta AK. Transmission length of pretensioned concrete systems – comparison of codes and test data. Mag Concr Res 2019;71(17): 881–93. https://doi.org/10.1680/jmacr.17.00553.
[41] ASTM A416. Standard specification for low-relaxation, seven-wire steel strand for prestressed concrete. West Conshohocken, PA, USA: ASTM International; 2016.
[42] Mohandoss P, Pillai RG, Gettu R. Effect of prestress on the bond strength of pretensioned concrete systems. 3rd N. Raikar Memorial International Conference & Gettu-Kodur International Symposium on Advances in Science & Technology of Concrete. 2018.
[43] ASTM C192,. Standard practice for making and curing concrete test specimens in the laboratoy. West Conshohocken, PA, USA: ASTM International; 2016.
[44] Benítez JoséM, Gálvez JC. Bond modelling of prestressed concrete during the prestressing force release. Mater Struct 2011;44(1):263–78.